7100 *Biochemistry* **2010,** *49,* 7100–7107
DOI: 10.1021/bi100583x

BIOCHEMISTRY
including biophysical chemistry & molecular biology
Article

A Disulfide-Linked Amyloid-β Peptide Dimer Forms a Protofibril-like Oligomer through a Distinct Pathway from Amyloid Fibril Formation

Takahiro Yamaguchi,[‡] Hisashi Yagi,[§] Yuji Goto,[§] Katsumi Matsuzaki,[‡] and Masaru Hoshino*[,‡]

[‡]*Graduate School of Pharmaceutical Sciences, Kyoto University, 46-29 Yoshida-Shimoadachi, Sakyo-ku, Kyoto 606-8501, Japan, and* [§]*Institute for Protein Research, Osaka University, 3-2 Yamadaoka, Suita, Osaka 565-0871, Japan*

Received April 16, 2010; Revised Manuscript Received July 9, 2010

ABSTRACT: The conversion of the soluble, nontoxic amyloid-β (Aβ) peptide into an aggregated, toxic form rich in β-sheets is considered a key step in the development of Alzheimer's disease. Whereas growing evidence indicates that the Aβ amyloid fibrils consist of in-register parallel β-sheets, little is known about the structure of soluble oligomeric intermediates because of their transient nature. To understand the mechanism by which amyloid fibrils form, especially the initial development of the "nucleus" oligomeric intermediates, we prepared covalently linked dimeric Aβ peptides and analyzed the kinetics of the fibril-forming process. A covalent bond introduced between two Aβ molecules dramatically facilitated the spontaneous formation of aggregates with a β-sheet structure and affinity for thioflavin T. Transmission electron microscopy revealed, however, that these aggregates differed in morphology from amyloid fibrils, more closely resembling protofibrils. The protofibril-like aggregates were not the most thermodynamically stable state but were a kinetically trapped state. The results emphasize the importance of the conformational flexibility of the Aβ molecule and a balance in the association and dissociation rate for the formation of rigid amyloid fibrils.

Alzheimer's disease (AD)[1] is a progressive neurodegenerative disorder. One of its pathological hallmarks is the extracellular deposition of senile plaques in the brain. The major component of these plaques is fibrillar aggregates (amyloid fibrils) of amyloid β-protein (Aβ), which is generated from the proteolytic cleavage of amyloid precursor protein (APP) by β- and γ-secretases (*1*, *2*). The conversion of soluble, nontoxic Aβ into an aggregated, toxic form rich in β-sheets is considered the key step in the development of AD. It is essential to elucidate the mechanisms by which Aβ aggregates to understand the pathogenesis of AD.

The most convincing model for the formation of amyloid fibrils is the nucleation-dependent polymerization model (*3*−*6*), which separates the fibrillization process into a nucleation phase and an elongation phase. Nucleation requires the self-association of soluble monomers, which is thermodynamically unfavorable and so rarely occurs. Once the nucleus is formed, however, the further addition of monomers is a much more favorable process and proceeds rapidly. As a result, the kinetics of amyloid fibril formation is well represented by a sigmoidal shape with a long lag phase followed by a rapid growth phase. Although the nucleation is a critical step in the development of amyloid fibrils, the precise mechanism involved is unknown because of its transient nature.

Extensive structural analyses of "mature" amyloid fibrils have been performed and a variety of models for the molecular organization of amyloid fibrils proposed (*7*, *8*). The "cross-β" structure is considered one of the most convincing models, where each molecule assumes a predominantly β-sheet structure which runs perpendicular to the fibril axis (*9*−*11*). In addition, recent studies with solid-state NMR spectroscopy suggest that the amyloid fibrils formed by partial or full-length Aβ-(1−40) and Aβ-(1−42) peptides are predominantly composed of in-register, parallel β-sheets although several variations in molecular organizations have been identified (*12*−*18*). These structural analyses suggest that while the C-terminal part of the Aβ molecule assumes a rigid structure in the fibrils, the N-terminal appears to be relatively flexible. In particular, Petkova et al. (*16*, *17*) showed that Aβ-(1−40) adopts a strand−turn−strand conformation and approximately the first 10 residues of the molecule are structurally disordered in the fibrils. This is also supported by analyses of H/D exchange detected with solution NMR spectroscopy (*19*, *20*).

To understand the mechanism by which amyloid fibrils form, especially the initial development of the "nucleus" oligomeric intermediates, we prepared covalently linked dimeric Aβ peptides and analyzed the kinetics of the fibrillation process. A covalent bond introduced between two Aβ molecules dramatically facilitated the spontaneous formation of ThT-active aggregates. Transmission electron microscopy (TEM) revealed, however, that these aggregates differed in morphology from amyloid fibrils, more closely resembling protofibrils. The protofibril-like aggregate was not the most thermodynamically stable state but was a kinetically trapped state. The results emphasize the importance of the dynamic flexibility of the Aβ molecule and a balance in the association and dissociation rate for the formation of rigid amyloid fibrils.

*Corresponding author. Phone: +81-75-753-4531. Fax: +81-75-753-4529. E-mail: hoshi@pharm.kyoto-u.ac.jp.

[1]Abbreviations: AD, Alzheimer's disease; Aβ, amyloid-β peptide; A2C-monomer, mutant Aβ(1−40) in which the second N-terminal Ala is replaced by Cys; A2C-dimer, disulfide-bonded homodimeric form of A2C-Aβ peptide; G_3C-monomer, mutant Aβ(1−40) in which an extra Cys residue is attached via a three-Gly linker; G_3C-dimer, disulfide-bonded homodimeric form of G_3C-Aβ peptide; ThT, thioflavin T; TEM, transmission electron microscopy; DTT, dithiothreitol; CD, circular dichroism; NMR, nuclear magnetic resonance; YUH-1, yeast ubiquitin hydrolase-1; SEC, size exclusion chromatography; ESI-MS, electrospray ionization mass spectrometry; FITC, fluorescein isothiocyanate.

 Published on Web 07/11/2010

MATERIALS AND METHODS

Construction of Expression Vectors. The expression vectors for wild-type and mutant Aβ-(1−40) peptides were constructed as an ubiquitin extension (*21*). A plasmid encoding the human ubiquitin gene was kindly provided by Dr. Gottfried Otting (Australian National University). A DNA fragment encoding ubiquitin was amplified by PCR to introduce an N-terminal hexahistidine tag and recognition sites for restriction enzymes with the primers 5′-TTTTTTTTCATATGCATCACCATCACCATCACGGCGGTGGCATGCAGATCTTCGTGAAGACTCTGAC-3′ and 5′-TTTGAATTCTTATCCACCTCTTAAGCGGAGTACCAGGTGCAGGG-3′ (the restriction sites for *Nde*I, *Eco*RI, and *Bsp*TI are underlined). The amplified DNA fragment was digested by *Nde*I and *Eco*RI and cloned into the vector pET28a (Novagen) to generate pET28a-H6Ub. Complementary oligonucleotide pairs (fA1 + rA1, fA2 + rA2, fA3 + rA3), each of which was phosphorylated at the 5′ end by T4 polynucleotide kinase, were annealed to produce three partially overlapping double-stranded DNA fragments (fA1, 5′-TTAAGAGGTGGAGATGCGGAATTTCGCCATGACAGCGGC-3′; rA1, 5′-TGATGAACCTCATAGCCGCTGTCATGGCGAAATTCCGCATCTCCACCTC-3′; fA2, 5′-TATGAGGTTCATCACCAGAAACTGGTGTTCTTTGCCGAAGATGTGGGT-3′; rA2, 5′-TGCACCTTTATTCGAACCCACATCTTCGGCAAAGAACACCAGTTTCTGG-3′; fA3, 5′-TCGAATAAAGGTGCAATCATTGGGCTGATGGTCGGCGGCGTTGTGTAAG-3′; rA3, 5′-AATTCTTACACAACGCCGCCGACCATCAGCCCAATGAT-3′). The annealed DNA fragments were ligated by T4 DNA ligase to generate an entire Aβ gene with restriction sites for *Bsp*TI and *Eco*RI at both termini. The Aβ gene was inserted into a pET28a-H6Ub vector between *Bsp*TI and *Eco*RI sites to construct pET28a-H6UbAβ-(1−40). The plasmids encoding mutant Aβ peptides, in which Ala2 was replaced by Cys or an extra Cys residue was added at the C-terminus via a three-Gly linker, were constructed by the QuickChange (Stratagene) method using pET28a-H6UbAβ-(1−40) as a template DNA.

Expression and Purification of Proteins. The expression vectors encoding wild-type and mutant ubiquitin-Aβ-(1−40) fusion protein were transformed into *Escherichia coli* strain BL21(DE3)/pLysS (Novagen). Transformed bacteria were grown at 37 °C in Lucia broth medium containing 25 μg/mL of kanamycin. Isopropyl β-D-thiogalactopyranoside (IPTG) was added to the medium when the absorbance at 600 nm reached 0.6. After 3 h, cells were harvested by centrifugation at 5000*g* for 15 min at 4 °C. Wild-type and mutant H6UbAβ-(1−40) proteins were accumulated in inclusion bodies and purified as follows. The bacterial cells were suspended into buffer A (300 mM NaCl, 50 mM sodium phosphate, pH 8.0) containing 1 mM phenylmethylsulfonyl fluoride and disrupted by sonication with intermittent pulses for 1 min (pulse of 0.5 s, interval of 0.5 s, output level of 7) by three times using an ultrasonic disruptor equipped with a TP-012 standard tip (UD-201; Tomy, Tokyo). After centrifugation at 10000*g* for 60 min at 4 °C, the pellet was collected and washed twice with buffer A. The pellet was then dissolved in buffer A containing 8 M urea and 20 mM imidazole and loaded onto HisTrap FF (GE Healthcare). After the column was washed with buffer A containing 20 mM imidazole, bound protein was eluted with buffer A containing 500 mM imidazole.

The plasmid encoding hexahistidine-tagged yeast ubiquitin hydrolase-1 (YUH-1) was kindly provided by Dr. Yutaka Ito (Tokyo Metropolitan University). The vector was introduced into *E. coli* BL21(DE3)/pLysS, and the protein was induced to express by IPTG using the same procedure as for H6UbAβ-(1−40). The protein was expressed as a soluble form and purified from the supernatant of cell lysate prepared by the same protocols of sonication and centrifugation as for H6UbAβ-(1−40). The supernatant was collected and loaded onto HisTrap FF. After the column was washed with buffer A containing 20 mM imidazole, bound protein was eluted with buffer A containing 500 mM imidazole. Purified protein was dialyzed against 0.5 mM EDTA and 50 mM Tris-HCl, pH 7.5 (buffer B) and stored at −20 °C in buffer B containing 50% glycerol.

Wild-type and mutant Aβ-(1−40) peptides were obtained by the proteolytic cleavage of H6UbAβ-(1−40) by YUH-1. Purified proteins were incubated for 1 h at 37 °C at a molar ratio of H6UbAβ-(1−40):YUH1 = 10:1. The cleaved Aβ-(1−40) moiety was purified by reversed-phase HPLC using a Protein-R packed column (Nacalai Tesque, Kyoto) with a linear gradient of acetonitrile. The fraction containing Aβ-(1−40) was collected and lyophilized. Cys-containing Aβ-(1−40) mutants were dimerized by thiol oxidation. To minimize the self-aggregation of peptides during the reaction, oxidation was performed in 95% dimethyl sulfoxide and 2% acetic acid for 1 week at 25 °C (*22*, *23*). Oxidized peptides were purified by reversed-phase HPLC. The purity and identity of the peptides were confirmed by analytical reversed-phase HPLC and electrospray ionization mass spectrometry. The purity of the peptides was greater than 95%.

Seed-Free Aβ Preparation. Purified Aβ peptides were dissolved in 0.02% ammonia on ice, and any large aggregates that could potentially induce amyloid fibrils to form were removed by ultracentrifugation in 500 μL polyallomer tubes at 540000*g*, 4 °C, for 3 h. A supernatant fraction was collected, and the concentration of peptide was determined in triplicate by Micro BCA protein assay (Pierce, Rockford, IL). The concentrations of disulfide-linked dimers are described as those corresponding to the monomer. The supernatant was stored as a stock solution at −80 °C prior to use. Just before the experiment, the stock solution of each Aβ was mixed with an equal volume of double concentrated PBS (16.0 g/L NaCl, 0.40 g/L KCl, 2.30 g/L Na_2HPO_4, and 0.40 g/L KH_2PO_4, pH 7.4). In the case of disulfide-reduced monomeric peptides, 5 mM dithiothreitol (DTT) was added to prevent the oxidation of sulfhydryl groups during experiments.

Size Exclusion Chromatography (*SEC*). The oligomeric state of Aβ peptides was analyzed by size exclusion chromatography using a column of Superdex 75 10/300 GL with an exclusion limit of 42000 Da (GE Healthcare), which had been pretreated with an excess of bovine serum albumin to block the nonspecific binding of proteins. Fifty microliters of each sample (15 μM) was injected into the column equilibrated with PBS, pH 7.4, at a flow rate of 0.5 mL/min and detected by the absorbance at 220 nm. Molecular weight was estimated with FITC-dextrans (MW 4400, 21200, and 42000) as standards (*24*).

Thioflavin T Fluorescence. The kinetics of the aggregation of Aβ peptides was monitored as the increase in fluorescence of thioflavin T (ThT) (*6*). The peptide stock solutions dissolved in 0.02% ammonia were mixed with the same volume of double concentrated PBS on ice and further diluted by PBS to prepare a 15 μM sample solution. The sample temperature was raised to 37 °C to initiate the reaction. After various periods of time, an aliquot of 66.7 μL was added to 1.93 mL of 5 μM ThT solution in

Table 1: Amino Acid Sequences and Molecular Weights of Aβ Peptides

abbreviation	sequence[a]	MW calcd[b]	MW exptl[c]
wild type	DAEFRHDSGYEVHHQKLVFFAEDVGSNKGAIIGLMVGGVV	4329.7	4329.9 ± 0.4
A2C-monomer	D**C**EFRHDSGYEVHHQKLVFFAEDVGSNKGAIIGLMVGGVV	4361.8	4362.0 ± 0.4
A2C-dimer	D**C**EFRHDSGYEVHHQKLVFFAEDVGSNKGAIIGLMVGGVV | D**C**EFRHDSGYEVHHQKLVFFAEDVGSNKGAIIGLMVGGVV	8721.5	8721.9 ± 0.8
G_3C-monomer	DAEFRHDSGYEVHHQKLVFFAEDVGSNKGAIIGLMVGGVV**GGGC**	4604.0	4604.0 ± 0.1
G_3C-dimer	DAEFRHDSGYEVHHQKLVFFAEDVGSNKGAIIGLMVGGVV**GGGC** | DAEFRHDSGYEVHHQKLVFFAEDVGSNKGAIIGLMVGGVV**GGGC**	9206.0	9205.9 ± 0.7

[a]Mutated residues are indicated by bold type and underlined. [b]Based on amino acid composition with isotope averaging. [c]Determined by ESI-MS.

50 mM glycine−NaOH buffer, pH 8.5. Fluorescence at 490 nm was measured at an excitation wavelength of 446 nm on a Shimadzu RF-5300 spectrofluorometer with a cuvette holder thermostated at 25 °C. To prepare the seeds for the amyloid fibrils, spontaneously formed aggregates were sonicated on ice with 20 intermittent pulses (pulse of 0.6 s, interval of 0.4 s, output level of 2) using an ultrasonic disruptor equipped with a TP-030 microtip (UD-201; Tomy, Tokyo). Sonicated seed fibrils at 5% (w/w) were added to seed-free Aβ peptides.

Circular Dichroism (CD). CD spectra were measured at 37 °C on a Jasco J-820 spectropolarimeter with a 1 mm path length quartz cell to minimize the absorbance due to buffer components. The results are expressed as mean residue ellipticity [θ]. Eight scans were averaged for each sample.

TEM. TEM experiments were carried out by the Ultrastructure Research Institute of Hanaichi Co. Ltd. (Okazaki, Japan). Samples were spread on carbon-coated grids, negatively stained with uranyl acetate, and examined under a JEOL JEM2000EX electron microscope with an acceleration voltage of 100 kV.

RESULTS

Design and Characterization of Mutant Aβ Peptides. The formation of amyloid fibrils generally requires the self-association of monomeric proteins, and there is growing evidence that the Aβ amyloid fibrils consist of in-register parallel β-sheets. Based on kinetic and structural models, we speculated that fibril-forming process would be facilitated by covalently linking two Aβ molecules in a parallel orientation through disulfide bonds at the N- or C-termini. We chose the second N-terminal residue as a site for substitution and produced an Ala2Cys mutant, because replacement of the N-terminal Asp residue with Cys might significantly affect physicochemical properties due to a change in the net charge of the molecule. To evaluate the effect of introducing the disulfide linker at a particular site, another control peptide was prepared. In this mutant, an additional Cys residue was introduced at the C-terminus with a preceding three-Gly linker sequence to minimize the effect of mutation and cross-linking because the C-terminal part of the Aβ molecule is considered to be rigid in amyloid fibrils. Amino acid sequences of the mutant Aβ peptides are summarized in Table 1.

Each Aβ peptide obtained as a fusion protein with ubiquitin was digested by YUH-1 to cleave between ubiquitin and the Aβ moiety and purified by reversed-phase HPLC. Cysteine-containing mutants were then oxidized to produce dimeric species linked by disulfide bonds. A long incubation of Aβ peptides under aqueous conditions often leads to the irreversible formation of amyloid fibrils. Therefore, we performed the oxidization of the cysteine side chain in the presence of a high concentration of dimethyl sulfoxide. This mild organic solvent is known to act as an oxidant (*22*) and, more importantly, effectively dissolves amyloid fibrils into monomeric molecules (*25*). By performing the oxidation reaction in dimethyl sulfoxide, we obtained oxidized dimeric peptides in high yield. Reversed-phase HPLC revealed that the retention time of the dimeric peptide was significantly longer than that of the monomeric counterpart, indicating that the hydrophobicity of the molecule increased upon dimerization (Figure 1). It was confirmed by reversed-phase HPLC and ESI-MS analyses that the expected monomeric and dimeric species were obtained with a purity of more than 95% (Table 1).

Oligomeric State of Aβ Peptides. The oligomeric forms of the wild-type and mutant Aβ peptides were examined under aqueous conditions by size exclusion chromatography (Figure 2). Seed-eliminated Aβ solutions were loaded onto a column of Superdex 75 equilibrated with PBS. The wild-type and A2C-dimer Aβ were eluted as a single peak at 26.5 and 23.3 min, respectively. By using FITC-dextrans as a standard, the apparent molecular weight of the wild type and A2C-dimer was estimated to be 4870 and 8240, respectively. These values corresponded well to the monomeric and dimeric forms of Aβ, indicating that each peptide dispersed well under near physiological conditions, and no accumulation of higher oligomeric species was detected. Similar results were also obtained for the other mutant peptides (data not shown).

Spontaneous Aggregation of the A2C-Dimer. Spontaneous aggregation of the wild-type and mutant Aβ peptides was monitored as increases in the fluorescence intensity of the amyloid-specific dye ThT. As shown in Figure 3, no increase in ThT fluorescence was observed for the wild type and A2C-monomer for up to 6 h at 37 °C. Longer incubation for 7 days, however, resulted in a significant increase in fluorescence as typically observed for the spontaneous amyloid formation of Aβ-(1−40) with a long lag phase. In contrast, a rapid increase in fluorescence without any detectable lag phase was observed when the A2C-dimer was incubated. It is evident that the aggregation of Aβ peptide was significantly facilitated by disulfide bonds. The disappearance of the lag phase suggests that the disulfide bond of two separate molecules dramatically reduced high energetic barrier that usually separates soluble monomers from spontaneously formed aggregates. The aggregation kinetics of the A2C-dimer were fitted to a single exponential curve with an apparent rate constant of 0.74 ± 0.06 (h^{-1}). Although the aggregation was

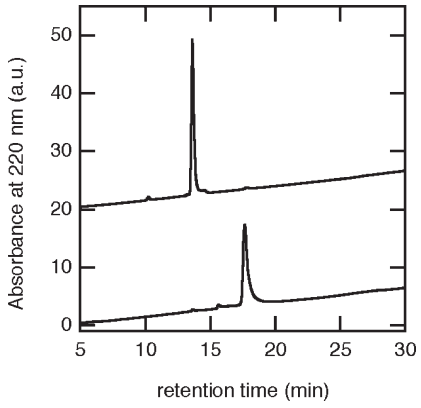

FIGURE 1: Reversed-phase HPLC profiles of the A2C-monomer (upper) and A2C-dimer (lower). Ten micrograms of the A2C-monomer and A2C-dimer was loaded onto a Protein-R packed column. Each peptide was eluted with a linear gradient of acetonitrile (25−50% acetonitrile for 30 min). The retention time of the A2C-monomer and A2C-dimer was 13.6 and 17.7 min, respectively.

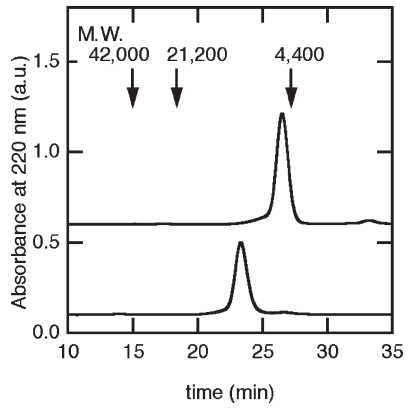

FIGURE 2: Elution profiles of size exclusion chromatography of the wild type (upper) and A2C-dimer (lower). Fifty microliters of 15 μM wild-type and A2C-dimer peptides dissolved in PBS (pH 7.4) was loaded onto a Superdex 75 10/300 GL column. The elution positions of FITC-dextrans used as molecular weight standards are indicated by arrows. The molecular weight of the wild type and A2C-dimer was estimated to be 4870 and 8240, respectively.

decelerated by lowering either the peptide concentration or temperature during the incubation period, all of the kinetics were exhibited as single exponential curves, and no lag phase was observed (data not shown).

Secondary Structural Analysis. To elucidate the secondary structural change upon oligomerization detected using ThT, far-UV CD spectra were measured before and after incubation at 37 °C (Figure 4). The spectrum of the wild-type peptide recorded prior to the incubation showed a characteristic minimum at 200 nm, indicating that the peptide assumed a random-coil conformation. After a long incubation, the spectrum changed significantly to exhibit a broad minimum at 218 nm, confirming the formation of amyloid fibrils rich in β-sheets. A similar conformational change was observed for the A2C-dimer but on a much shorter time scale (Figure 4B). After an incubation period of 1 day, the spectrum obtained was very similar to that of wild-type peptides recorded after a long incubation. The results indicate that a similar conformational change occurred in both the wild-type and A2C-dimer peptides. However, the spectrum of the mutant recorded without incubation was slightly different from that of the wild type, indicating the presence of both

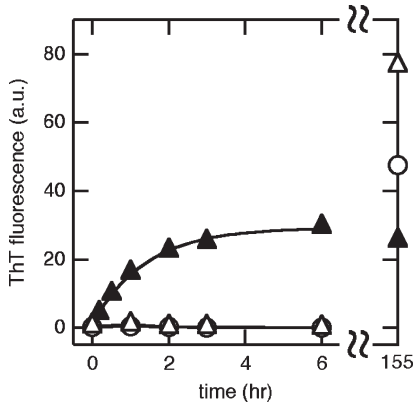

FIGURE 3: Spontaneous aggregation by N-terminal mutant Aβ peptides monitored using ThT fluorescence. Each peptide solution (15 μM) in PBS (pH 7.4) prepared on ice was incubated at 37 °C. After various periods of time, an aliquot of 66.7 μL was added to 1.93 mL of 5 μM ThT solution in 50 mM glycine−NaOH buffer, pH 8.5. Fluorescence at 490 nm was measured at an excitation wavelength of 446 nm at 25 °C. Key: open circle, wild type; open triangle, A2C-monomer; closed triangle, A2C-dimer.

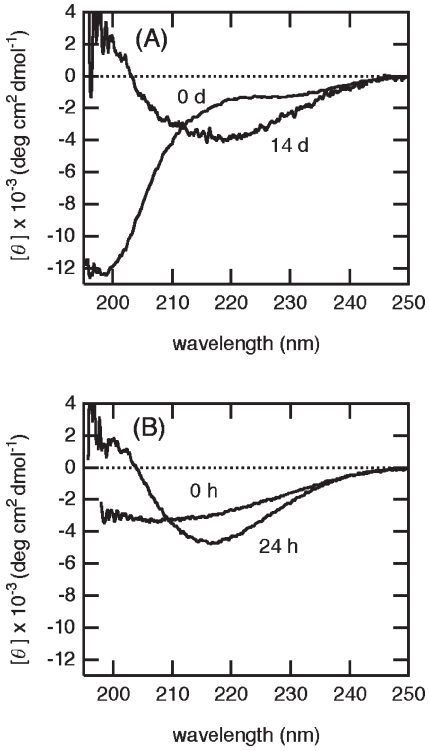

FIGURE 4: CD spectra of the wild-type (A) and A2C-dimer mutant (B) Aβ peptides at 37 °C in PBS (pH 7.4). Each peptide solution prepared on ice was measured immediately after its preparation or measured after the incubation period indicated at 37 °C. The results are expressed as mean residue ellipticity [θ]. Eight scans were averaged for each sample.

random-coil and β-sheet conformations. This is probably due to the rapid formation of aggregates during the CD measurements (~30 min) as evidenced by the results of the ThT fluorescence analysis (Figure 3).

TEM Observation. To further characterize the aggregates formed by the wild-type and mutant Aβ peptides, their morphology was examined by TEM. The wild-type aggregates were found to have a long, nonbranched, straight filament structure with a diameter of 7−8 nm, demonstrating the formation of typical

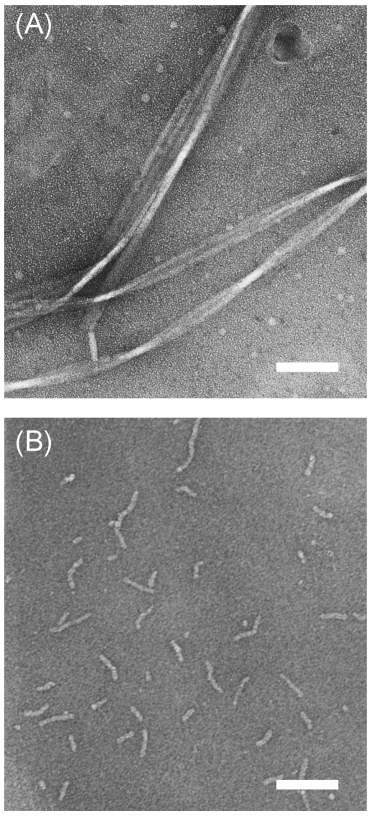

FIGURE 5: TEM images of spontaneously formed aggregates by wild-type (A) and A2C-dimer mutant (B) Aβ peptides. Each peptide solution (15 μM) incubated at 37 °C was spread on carbon-coated grids, negatively stained with uranyl acetate, and examined under a JEOL JEM2000EX electron microscope with an acceleration voltage of 100 kV. Scale bar: 100 nm.

amyloid fibrils (Figure 5A). On the other hand, the aggregate formed by the A2C-dimer had a very different morphology (Figure 5B). These aggregates had a short, curved structure, and their morphology closely resembled that of protofibrils, which were proposed to be a precursor for the amyloid fibril (*26*−*29*). Although it is not clear whether the protofibril-like aggregates formed by the A2C-dimer are the on-pathway intermediates in the formation of amyloid fibrils, they did not change into the amyloid fibrils at least under the conditions examined.

Cross-Seeding Assay. The A2C-dimer peptide rapidly formed aggregates with characteristics of amyloid fibrils such as the specific binding of ThT and a predominantly β-sheet conformation, and therefore the molecular organization could be similar. On the other hand, TEM revealed that their overall morphology was strikingly different from that of typical amyloid fibrils. As a stringent test of the identity of the molecular assemblies formed by different molecular species, we performed cross-seeding assays (Figure 6). The aggregates spontaneously formed by the wild-type, A2C-monomer, and A2C-dimer peptides were sonicated and added to a seed-eliminated solution of the wild-type peptide. The addition of a small amount of preformed amyloid fibrils formed by the wild-type peptide dramatically increased the rate of fibrillation, resulting in the disappearance of the lag phase. The same result was obtained when the sonicated aggregate formed by the A2C-monomer was added to the seed-eliminated wild-type peptide solution. These results indicate that the aggregate formed by the A2C-monomer acts as a seed for amyloid fibrils of the wild-type peptide and that the replacement of Ala with Cys at position 2 did not affect the

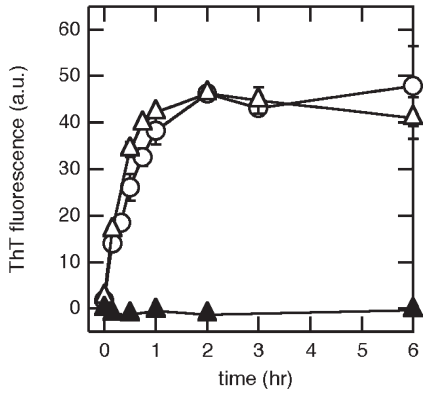

FIGURE 6: Analysis of cross-seeding activity of N-terminal Aβ mutants. Seeds were prepared by sonicating spontaneously formed aggregates of each peptide and were added at 5% (w/w) to seed-free wild-type Aβ solution. After various incubation periods at 37 °C, an aliquot of sample was analyzed using ThT fluorescence. Key: open circle, wild type; open triangle, A2C-monomer; closed triangle, A2C-dimer.

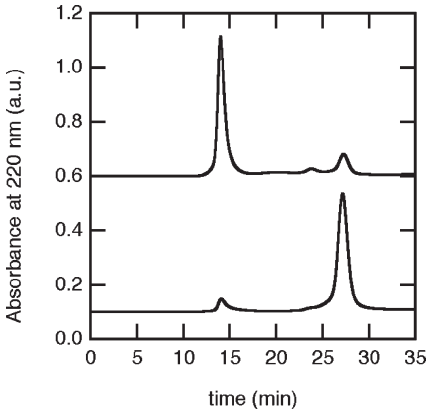

FIGURE 7: Reversible dissociation from protofibril-like aggregates into the A2C-monomer. Elution profiles of size exclusion chromatography of A2C-dimer aggregates immediately (upper) and 1.5 h (lower) after treatment with 5 mM DTT. Fifty microliters of the solution was loaded onto a Superdex 75 10/300 GL column equilibrated with PBS, pH 7.4, at a flow rate of 0.5 mL/min, and the proteins were detected by absorbance at 220 nm.

structure or formation of amyloid fibrils. In contrast, no increase in ThT fluorescence was observed for up to 6 h when the preformed aggregate of the A2C-dimer was added to the solution. This indicates that the protofibril-like aggregate formed by the A2C-dimer does not act as a seed for the wild-type peptide, reflecting the difference in molecular organization from the amyloid fibrils formed by the wild-type peptide and A2C-monomer.

Reversible Dissociation from Protofibril-like Aggregates. While the aggregate formed by the A2C-monomer could act as a seed for extension of the wild-type peptide, the disulfide-linked A2C-dimer was found to form aggregates with a protofibril-like morphology but no seeding activity for wild-type peptides. To elucidate whether it is possible to convert the protofibril-like aggregate of the A2C-dimer into that of the A2C-monomer with seeding activity and whether the N-terminal region is accessible to solvent, the reactivity of preformed aggregates against a reducing reagent was examined. Surprisingly, the incubation of A2C-dimer aggregates in the presence of 5 mM DTT resulted in the disappearance of the void fraction in the SEC profile and concomitantly eluted as a single peak at

27.0 min, corresponding to the A2C-monomer (Figure 7, compared with Figure 2). In addition, NMR measurements in solution confirmed that the aggregates preformed by the A2C-dimer dissociated reversibly into a soluble monomeric form judging from the fine line width of resonances (Supporting Information Figure S1). These results demonstrated that while the A2C-dimer changed rapidly into a protofibril-like aggregate, it reversibly dissociated into the soluble monomeric form upon disulfide reduction. This indicates that the disulfide bond located at the N-terminus is readily accessible to solvent and, more importantly, stabilizes the protofibril-like aggregates spontaneously formed by the A2C-dimer.

G_3C-Dimer. The results indicated that while substitution of the N-terminal Ala with Cys did not affect the formation of amyloid fibrils, dimerization via disulfide linkage prevented amyloid fibril formation by themselves as well as interaction with the wild-type peptide. To elucidate whether the effect of disulfide bonds on amyloid fibrils is site-specific, we examined the ability of the C-terminal-linked dimer to form fibrils. Whereas the N-terminal region is indicated to be flexible and exposed to solvent in amyloid fibrils, modification at the C-terminal could severely affect the aggregating property as exemplified by the difference between Aβ-(1−40) and Aβ-(1−42) (*30*, *31*). Therefore, we added an extra Cys residue at the C-terminus via a three-Gly linker sequence to minimize the effect of the mutation.

As shown in Supporting Information Figure S2, no increase in ThT fluorescence was detected for up to 6 h when the G_3C-monomer was incubated at 37 °C, indicating that spontaneous aggregation did not occur similar to the case for the wild-type peptide and A2C-monomer. In contrast, the disulfide-linked dimeric form, the G_3C-dimer, exhibited a rapid increase in ThT fluorescence. Similar to the N-terminal-linked dimer, the process was well represented by a single exponential curve with an apparent rate constant of 2.92 ± 0.40 (h^{-1}). The G_3C-dimer also formed aggregates rich in β-sheets as determined by CD spectroscopy (data not shown). In addition, the morphology of the aggregates formed by G3C-dimer was very similar to those formed by A2C-dimer peptides (Supporting Information Figure S3). These results suggest that a covalent bond at either terminus facilitates aggregation regardless of its position.

Next, we examined whether these G_3C aggregates have seeding activity for amyloid fibrils of the wild-type Aβ peptide (Supporting Information Figure S4). As was the case for the A2C-species, while the aggregate formed by the G_3C-monomer acted as a seed for amyloid fibrils of the wild-type peptide, eliminating a lag phase in the kinetics, no activity was evident in the case of the G_3C-dimer.

DISCUSSION

In this study, we prepared disulfide-linked Aβ dimeric peptides and analyzed the kinetics of their aggregation and their structural properties. Spontaneous aggregation was clearly facilitated in the Aβ dimers, resulting in a rapid increase in ThT fluorescence without a lag period. These results support the nucleation-dependent polymerization model for the formation of amyloid fibrils. According to this model, the lag phase is caused by a series of association events involving Aβ molecules. Disulfide-linking between two separate molecules significantly increased the effective concentration, resulting in rapid aggregation. Indeed, it was shown that the length of the lag period depends on the protein concentration (*3*).

TEM revealed that the aggregates formed by the A2C-dimer, however, differed in morphology from amyloid fibrils. They were similar to protofibrils in morphology as well as several physicochemical properties (*28*, *29*). (1) The aggregates formed by Aβ dimers showed significantly lower values of ThT fluorescence than did the amyloid fibrils formed by Aβ monomers (Figure3). (2) They were not precipitated by centrifugation at 10000*g* for 10 min but were under more rigorous conditions, e.g., 200000*g* for 3 h (data not shown). In contrast, the protofibril-like aggregates found in this study did not act as a seed for the development of amyloid fibrils by the wild-type peptide. This suggests that the aggregates formed by Aβ dimers differ from amyloid fibrils in terms of their structural organization, although they share several physicochemical characteristics including CD spectra and ThT binding. It is, however, not clear whether the aggregates formed by Aβ dimers are the same as protofibrils, whose structural properties still remain to be elucidated. In addition, to our knowledge, there is no direct evidence demonstrating that protofibrils are the on-pathway intermediates in the formation of amyloid fibrils. An increasing number of molecular assemblies with a variety of size and shape have also been identified (*32*, *33*). Although the detailed structure of the protofibrillar-like aggregates found in this study is unknown, they did not change into the amyloid fibrils at least under the conditions examined.

We speculated that the cross-linking at the N-terminus of Aβ-(1−40) did not affect the amyloidogenic property based on evidence that N-terminal residues are highly flexible and exposed to solvent (*16*, *17*, *19*). One of the most straightforward explanations for the failure of the dimeric Aβ-(1−40) to form fibrils is steric hindrance introduced by the disulfide cross-link. Several reports indicate the possible role of the N-terminal part of the Aβ molecule in the development of amyloid fibrils. For example, Lim showed that the N-terminal region of Aβ-(1−40) was partially structured at low temperature and suggested that an increase in flexibility of the N-terminus triggers aggregation (*34*). It is possible that the N-terminal region of the A2C-dimer is structurally restricted by the introduction of disulfide linking, resulting in a failure of amyloid fibril formation. On the other hand, Zhang et al. (*35*) analyzed the amyloid fibrils of Aβ-(1−42) by cryo-EM and reconstructed a 3D model in which one protofilament interacts with another filament through the N-terminal residues. Therefore, any modification even at the N-terminus of the molecule could affect significantly the morphology of fibrils. It should also be mentioned that there are two negatively charged residues (Asp1 and Glu3) in the proximal to the N-termini, and the cross-linking at this site would not be compatible to the amyloid fibrils with in-resister parallel packing. Therefore, it might result in the different type of molecular organization from amyloid fibrils. However, it should be noted that another dimeric peptide, the G_3C-dimer, was found to have almost identical kinetic and structural properties to the N-terminally cross-linked dimer (Figures 3 and 6). In addition, the monomeric counterpart of each mutant peptide (A2C-monomer and G_3C-monomer) formed amyloid fibrils with seeding activity, and it has been shown that the fibrillation process is quite tolerant of the amino acid substitution (*36*−*38*).

Schmechel et al. (*39*) prepared disulfide-linked dimers of Aβ-(1−40) and Aβ-(1−42) by substituting lysine 28 with a cysteine residue. They reported that the K28C homodimers also formed fibrils with a significantly increased β-sheet content compared to the corresponding monomers. Considering that K28 is thought to form a salt bridge with D23 in the amyloid

fibrils (*17*, *40*), it is surprising that the K28C mutants could form a fibrillar structure although its length and thickness differed from that of the wild-type peptide. It is unknown whether these fibrils could act as a seed for amyloid fibrils of the wild-type peptide. Considering the difference in morphology, however, these fibrils might be formed through different pathways from those of wild-type peptides. Although their results are apparently inconsistent with the present study, direct comparison is difficult because even wild-type Aβ-(1−40) peptide did not form amyloid fibrils but formed protofibrils under their experimental conditions.

Since oligomeric intermediate species form only temporarily, their structural details and mechanisms of formation remain to be elucidated. Chimon et al. (*41*) revealed that a spherical Aβ-(1−40) oligomeric intermediate (I_β), which consists of a parallel β-sheet similar to amyloid fibrils, was formed after a relatively long lag period. While they report I_β as an on-pathway intermediate, they also suggest that another intermediate lacking an ordered β-sheet arrangement (non-β intermediate: $I_{N\beta}$) is accumulated during the lag period preceding the formation of I_β, and that these two intermediates are in equilibrium. On the other hand, intermediate species with antiparallel β-sheet structures are also suggested. Hoyer et al. (*42*) revealed that monomeric Aβ-(1−40) complexed with affibody protein $Z_{A\beta3}$ adopted an antiparallel β-hairpin conformation and suggested that a structural reorganization of the plane of the strands by 90° would be required for conversion of the oligomer into fibrils. In addition, recent FTIR analyses revealed that whereas the fibrillar form of Aβ was represented by a parallel β-sheet conformation, a minor but significant amide I band at 1693−1695 cm^{-1}, which is attributed to an antiparallel β-sheet structure, was present in the oligomeric form of Aβ (*43*, *44*). Although further studies are needed to obtain a detailed molecular picture, dynamic rearrangements in each molecule might be necessary for the formation of mature amyloid fibrils. Disulfide linkage would interfere with such a conformation adopted temporally in the early stage of Aβ aggregation.

Another important factor which could affect the overall pathway is the kinetic control of each association event. The similarity between amyloid fibrils and crystals in structural regularity, the high energy barrier between different molecules, and the nucleus-dependent growth process is often emphasized (*9*). It is also known that too rapid a growth can result in many small crystals or amorphous aggregates, and the growth of "high-quality" crystals usually requires a slow, quasi-equilibrium process (*45*). The presence of a similar slow kinetic phase during the formation of amyloid fibrils is also predicted by the "dock-lock" mechanism, where a significant conformational change of monomeric molecules is necessary before being rigidly incorporated into preexisting fibrils (*46*). These observations emphasize the importance of the dynamic flexibility of Aβ molecules and a balance in the association and dissociation rate for the formation of mature long (large) fibrils (crystals). Multiple rounds of association and dissociation must occur during a long lag period observed in the kinetics of spontaneous fibrillation, and this process would be necessary to form a "seed" oligomer with a well-ordered structure. If, on the other hand, the molecule has too strong a tendency for self-association, it would fail to form a large, homogeneous organization, and instead form a nonspecific amorphous aggregate. We observed here that the dimeric form of Aβ-(1−40) did not produce typical amyloid fibrils with a long, straight morphology but spontaneously formed much shorter, protofibril-like curvy aggregates without any detectable lag period. Intriguingly, their monomeric counterparts formed mature amyloid fibrils with seeding activity for wild-type peptides. Although the amino acid composition of monomeric and dimeric peptides was identical, doubling the total number of amino acids in the polypeptide chain increased considerably the hydrophobicity as evidenced by the difference in retention time in reversed-phase chromatography (Figure1). Therefore, the dimeric peptides are expected to have a stronger tendency for self-association under the same conditions. Most importantly, the aggregates formed by the dimeric peptides were not thermodynamically stable, as demonstrated by the reversible dissociation of the molecules from preformed aggregates when they were incubated with a high concentration of DTT (Figure 7). Therefore, the aggregates formed by dimeric mutants represent a kinetically trapped state probably due to too strong a tendency for self-association. Our results suggests that greater hydrophobicity in the dimeric form may result in a loss of the appropriate balance of association and dissociation that is necessary for the growth of mature amyloid fibrils with structural regularity and homogeneity.

A similar mechanism has been proposed by Hong et al. (*47*), who showed that an amyloidogenic protein, β2-micloglobulin, spontaneously formed "immature fibrils" under conditions favoring self-association, such as in the presence of a high concentration of salt at acidic pH. While the morphology of immature fibrils resembled that of protofibrils, these fibrillar aggregates did not have seeding activity for amyloid fibrils but showed less β-sheet content and ThT activity than "mature" amyloid fibrils. They suggested that the greater tendency for self-association under the conditions would result in the failure to form rigid amyloid fibrils. Similarly, Ohhashi et al. (*48*) showed that a disulfide cross-linked dimer of the amyloidogenic peptide K3, corresponding to residues Ser20−Lys41 of β2-microglobulin, aggregated spontaneously without a lag phase to form amyloid fibrils under physiological conditions. The fibrils formed by the K3 dimer were, however, shorter than the monomeric fibrils. The authors considered the shorter fibrils produced by the K3 dimer to be related to the too strong potential to form fibrils.

In summary, we prepared a dimeric form of the Aβ-(1−40) peptide in which two molecules were cross-linked by N- or C-terminally introduced cysteine residues. While the monomeric form of both mutant peptides formed amyloid fibrils with seeding activity for the elongation of the wild-type peptide, the dimeric form of the peptides spontaneously associated to form thinner, curvy aggregates that resemble protofibrils. These protofibrillar aggregates did not act as a seed for amyloid fibril extension of the wild-type peptide, indicating a conformational difference from amyloid fibrils. Higher hydrophobicity and concomitant aggregation may kinetically control the reaction and alter the overall pathway, emphasizing the importance of a suitable balance of association and dissociation for the growth of amyloid fibrils with structural regularity and homogeneity.

SUPPORTING INFORMATION AVAILABLE

The aggregates formed by C-terminal mutant Aβ characterized by kinetic measurement by ThT fluorescence, AFM images, and cross-seeding assay. This material is available free of charge via the Internet at http://pubs.acs.org.

REFERENCES

1. Selkoe, D. J. (1994) Cell biology of the amyloid β-protein precursor and the mechanism of Alzheimer's disease. *Annu. Rev. Cell Biol. 10*, 373–403.

2. Hardy, J., and Selkoe, D. J. (2002) The amyloid hypothesis of Alzheimer's disease: Progress and problems on the road to therapeutics. *Science 297*, 353–356.
3. Jarrett, J. T., and Lansbury, P. T., Jr. (1992) Amyloid fibril formation requires a chemically discriminating nucleation event: Studies of an amyloidogenic sequence from the bacterial protein OsmB. *Biochemistry 31*, 12345–12352.
4. Jarrett, J. T., and Lansbury, P. T., Jr. (1993) Seeding "one-dimensional crystallization" of amyloid: A pathogenic mechanism in Alzheimer's disease and scrapie? *Cell 73*, 1055–1058.
5. Naiki, H., and Nakakuki, K. (1996) First-order kinetic model of Alzheimer's β-amyloid fibril extension in vitro. *Lab. Invest. 74*, 374–383.
6. Naiki, H., and Gejyo, F. (1999) Kinetic analysis of amyloid fibril formation. *Methods Enzymol. 309*, 305–318.
7. Perutz, M. F., Finch, J. T., Berriman, J., and Lesk, A. (2002) Amyloid fibers are water-filled nanotubes. *Proc. Natl. Acad. Sci. U.S.A. 99*, 5591–5595.
8. Nelson, R., and Eisenberg, D. (2006) Structural models of amyloid-like fibrils. *Adv. Protein Chem. 73*, 235–282.
9. Dobson, C. M. (1999) Protein misfolding, evolution and disease. *Trends Biochem. Sci. 24*, 329–332.
10. Inouye, H., Fraser, P. E., and Kirschner, D. A. (1993) Structure of β-crystallite assemblies formed by Alzheimer β-amyloid protein analogues: Analysis by x-ray diffraction. *Biophys. J. 64*, 502–519.
11. Sunde, M., Serpell, L. C., Bartlam, M., Fraser, P. E., Pepys, M. B., and Blake, C. C. F. (1997) Common core structure of amyloid fibrils by synchrotron X-ray diffraction. *J. Mol. Biol. 273*, 729–739.
12. Benzinger, T. L., Gregory, D. M., Burkoth, T. S., Miller-Auer, H., Lynn, D. G., Botto, R. E., and Meredith, S. C. (1998) Propagating structure of Alzheimer's β-amyloid$_{(10-35)}$ is parallel beta-sheet with residues in exact register. *Proc. Natl. Acad. Sci. U.S.A. 95*, 13407–13412.
13. Antzutkin, O. N., Balbach, J. J., Leapman, R. D., Rizzo, N. W., Reed, J., and Tycko, R. (2000) Multiple quantum solid-state NMR indicates a parallel, not antiparallel, organization of β-sheets in Alzheimer's β-amyloid fibrils. *Proc. Natl. Acad. Sci. U.S.A. 97*, 13045–13050.
14. Balbach, J. J., Petkova, A. T., Oyler, N. A., Antzutkin, O. N., Gordon, D. J., Meredith, S. C., and Tycko, R. (2002) Supramolecular structure in full-length Alzheimer's β-amyloid fibrils: Evidence for a parallel β-sheet organization from solid-state nuclear magnetic resonance. *Biophys. J. 83*, 1205–1216.
15. Lührs, T., Ritter, C., Adrian, M., Riek-Loher, D., Bohrmann, B., Döbeli, H., Schubert, D., and Riek, R. (2005) 3D structure of Alzheimer's amyloid-β(1−42) fibrils. *Proc. Natl. Acad. Sci. U.S.A. 102*, 17342–17347.
16. Petkova, A. T., Ishii, Y., Balbach, J. J., Antzutkin, O. N., Leapman, R. D., Delaglio, F., and Tycko, R. (2002) A structural model for Alzheimer's β-amyloid fibrils based on experimental constraints from solid state NMR. *Proc. Natl. Acad. Sci. U.S.A. 99*, 16742–16747.
17. Petkova, A. T., Yau, W.-M., and Tycko, R. (2006) Experimental constraints on quaternary structure in Alzheimer's β-amyloid fibrils. *Biochemistry 45*, 498–512.
18. Tycko, R., Sciarretta, K. L., Orgel, J. P. R. O., and Meredith, S. C. (2009) Evidence for novel β-sheet structures in Iowa mutant β-amyloid fibrils. *Biochemistry 48*, 6072–6084.
19. Whittemore, N. A., Mishra, R., Kheterpal, I., Williams, A. D., Wetzel, R., and Serpersu, E. H. (2005) Hydrogen−deuterium (H/D) exchange mapping of Aβ_{1-40} amyloid fibril secondary structure using nuclear magnetic resonance spectroscopy. *Biochemistry 44*, 4434–4441.
20. Olofsson, A., Sauer-Eriksson, A. E., and Öhman, A. (2006) The solvent protection of alzheimer amyloid-β-(1−42) fibrils as determined by solution NMR spectroscopy. *J. Biol. Chem. 281*, 477–483.
21. Lee, E. K., Hwang, J. H., Shin, D. Y., Kim, D. I., and Yoo, Y. J. (2005) Production of recombinant amyloid-β peptide 42 as an ubiquitin extension. *Protein Expression Purif. 40*, 183–189.
22. Otaka, A., Koide, T., Shige, A., and Fujii, N. (1991) Application of dimethylsulphoxide(DMSO)/trifluoroacetic acid(TFA) oxidation to the synthesis of cystine-containing peptide. *Tetrahedron Lett. 32*, 1223–1226.
23. Tam, J. P., Wu, C.-R., Liu, W., and Zhang, J.-W. (1991) Disulfide bond formation in peptides by dimethyl sulfoxide. Scope and applications. *J. Am. Chem. Soc. 113*, 6657–6662.
24. Päiviö, A., Jarvet, J., Gräslund, A., Lannfelt, L., and Westlind-Danielsson, A. (2004) Unique physicochemical profile of beta-amyloid peptide variant Aβ1−40E22G protofibrils: Conceivable neuropathogen in arctic mutant carriers. *J. Mol. Biol. 339*, 145–159.
25. Hoshino, M., Katou, H., Hagihara, Y., Hasegawa, K., Naiki, H., and Goto, Y. (2002) Mapping the core of the β_2-microglobulin amyloid fibril by H/D exchange. *Nat. Struct. Biol. 9*, 332–336.
26. Harper, J. D., Lieber, C. M., and Lansbury, P. T., Jr. (1997) Atomic force microscopic imaging of seeded fibril formation and fibril branching by the Alzheimer's disease amyloid-β protein. *Chem. Biol. 4*, 951–959.
27. Harper, J. D., Wong, S. S., Lieber, C. M., and Lansbury, P. T., Jr. (1997) Observation of metastable Aβ amyloid protofibrils by atomic force microscopy. *Chem. Biol. 4*, 119–125.
28. Walsh, D. M ., Lomakin, A., Benedek, G. B., Condron, M. M., and Teplow, D. B. (1997) Amyloid β-protein fibrillogenesis. Detection of a protofibrillar intermediate. *J. Biol. Chem. 272*, 22364–22372.
29. Walsh, D. M., Hartley, D. M., Kusumoto, Y., Fezoui, Y., Condron, M. M., Lomakin, A., Benedek, G. B., Selkoe, D. J., and Teplow, D. B. (1999) Amyloid β-protein fibrillogenesis. Structure and biological activity of protofibrillar intermediates. *J. Biol. Chem. 274*, 25945–25952.
30. Yan, Y., and Wang, C. (2006) Aβ42 is more rigid than Aβ40 at the C terminus: Implications for Aβ aggregation and toxicity. *J. Mol. Biol. 364*, 853–862.
31. Olofsson, A., Lindhagen-Persson, M., Sauer-Eriksson, A. E., and Öhman, A. (2007) Amide solvent protection analysis demonstrates that amyloid-β(1−40) and amyloid-β(1−42) form different fibrillar structures under identical conditions. *Biochem. J. 404*, 63–70.
32. Glabe, C. G. (2008) Structural classification of toxic amyloid oligomers. *J. Biol. Chem. 283*, 29639–29643.
33. Roychaudhuri, R., Yang, M., Hoshi, M. M., and Teplow, D. B. (2009) Amyloid β-protein assembly and Alzheimer disease. *J. Biol. Chem. 284*, 4749–4753.
34. Lim, K. H. (2006) A weakly clustered N terminus inhibits Aβ(1−40) amyloidogenesis. *ChemBioChem 7*, 1662–1666.
35. Zhang, R., Hu, X., Khant, H., Ludtke, S. J., Chiu, W., Schmid, M. F., Frieden, C., and Lee, J.-M. (2009) Interprotofilament interactions between Alzheimer's Aβ_{1-42} peptides in amyloid fibrils revealed by cryoEM. *Proc. Natl. Acad. Sci. U.S.A. 106*, 4653–4658.
36. Shivaprasad, S., and Wetzel, R. (2006) Scanning cysteine mutagenesis analysis of Aβ-(1−40) amyloid fibrils. *J. Biol. Chem. 281*, 993–1000.
37. Williams, A. D., Shivaprasad, S., and Wetzel, R. (2006) Alanine scanning mutagenesis of Aβ(1−40) amyloid fibril stability. *J. Mol. Biol. 357*, 1283–1294.
38. Kim, W., and Hecht, M. H. (2006) Generic hydrophobic residues are sufficient to promote aggregation of the Alzheimer's Aβ42 peptide. *Proc. Natl. Acad. Sci. U.S.A. 103*, 15824–15829.
39. Schmechel, A., Zentgraf, H., Scheuermann, S., Fritz, G., Pipkorn, R., Reed, J., Beyreuther, K., Bayer, T. A., and Multhaup, G. (2003) Alzheimer β-amyloid homodimers facilitate Aβ fibrillization and the generation of conformational antibodies. *J. Biol. Chem. 278*, 35317–35324.
40. Petkova, A. T., Leapman, R. D., Guo, Z., Yau, W.-M., Mattson, M. P., and Tycko, R. (2005) Self-propagating, molecular-level polymorphism in Alzheimer's β-amyloid fibrils. *Science 307*, 262–265.
41. Chimon, S., Shaibat, M. A., Jones, C. R., Calero, D. C., Aizezi, B., and Ishii, Y. (2007) Evidence of fibril-like β-sheet structures in a neurotoxic amyloid intermediate of Alzheimer's β-amyloid. *Nat. Struct. Mol. Biol. 14*, 1157–1164.
42. Hoyer, W., Grönwall, C., Jonsson, A., Stahl, S., and Härd, T. (2008) Stabilization of a β-hairpin in monomeric Alzheimer's amyloid-β peptide inhibits amyloid formation. *Proc. Natl. Acad. Sci. U.S.A. 105*, 5099–5104.
43. Habicht, G., Haupt, C., Friedrich, R. P., Hortschansky, P., Sachse, C., Meinhardt, J., Wieligmann, K., Gellermann, G. P., Brodhun, M., Götz, J., Halbhuber, K.-J., Röcken, C., Horn, U., and Fändrich, M. (2007) Directed selection of a conformational antibody domain that prevents mature amyloid fibril formation by stabilizing Aβ protofibrils. *Proc. Natl. Acad. Sci. U.S.A. 104*, 19232–19237.
44. Cerf, E., Sarroukh, R., Tamamizu-Kato, S., Breydo, L., Derclaye, S., Dufréne, Y. F., Narayanaswami, V., Goormaghtigh, E., Ruysschaert, J.-M., and Raussens, V. (2009) Antiparallel β-sheet: A signature structure of the oligomeric amyloid β-peptide. *Biochem. J. 421*, 415–423.
45. Luft, J. R., and DeTitta, G. T. (1997) Kinetic aspects of macromolecular crystallization. *Methods Enzymol. 276*, 110–131.
46. Esler, W. P., Stimson, E. R., Jennings, J. M., Vinters, H. V., Ghilardi, J. R., Lee, J. P., Mantyh, P. W., and Maggio, J. E. (2000) Alzheimer's disease amyloid propagation by a template-dependent dock-lock mechanism. *Biochemistry 39*, 6288–6295.
47. Hong, D.-P., Gozu, M., Hasegawa, K., Naiki, H., and Goto, Y. (2002) Conformation of β_2-microglobulin amyloid fibrils analyzed by reduction of the disulfide bond. *J. Biol. Chem. 277*, 21554–21560.
48. Ohhashi, Y., Hasegawa, K., Naiki, H., and Goto, Y. (2004) Optimum amyloid fibril formation of a peptide fragment suggests the amyloidogenic preference of β_2-microglobulin under physiological conditions. *J. Biol. Chem. 279*, 10814–10821.